

# Research of Helicopter Tail Rotor Noise in the Regime of Axial Streamline.

**Samokhin V.F. (GosNITs TsAGI, Moscow),  
Animitsa V.A. (TsAGI, Zhukovsky, Moscow region),  
Rozhdestvensky M.G.(M.L.Mil Moscow Helicopter Plant)**

## **Abstract**

The work considers some results of parametric experimental research of acoustic characteristics of Mi-8 helicopter tail rotor at axial streamline, realized with the use of aerodynamic stand of M.L.Mil Moscow Helicopter Plant. In particular, the effect of blade sweep and of aerodynamic profile type, of thrust, rotor pitch, of peripheral velocity Mach number and blade loading on the propeller noise is examined.

## **Introduction.**

Community noise levels of civil helicopters are limited by maximum accepted values set in the ICAO standard [1] and in national airworthiness regulations for air vehicles (FAR36 in USA, JAR36 in the countries of EC and AP36 in Russia). Existence of these regulations and negative reaction of the community to helicopter operations within town-building regions causes to search for possible methods of reducing the unfavourable effect of helicopters on the environment. In this connection it is actual to study helicopter community noise sources and to acquire experimental data on noise mechanisms and regularities.

Aerodynamic sources of helicopter noise were first investigated in the 1960's and these investigations were based on the results of studying propeller rotation noise and fan vortex noise [2,3]. The principal mechanisms of noise generation by helicopter rotor were determined already in the first works on this subject [4]. A number of experimental and theoretical investigations made in the 1970-1980's years and partly presented in reviews [5,6],

were related to studying separate components of main rotor (MR) and tail rotor (TR) noise with sound pressure spectra, discrete and continuous in frequency.

In the early 1990's the important role of tail rotor in broad-band noise generation was established experimentally [7,8], methods of reducing the intensity of the dominating noise source of the helicopter rotor in the case of single-rotor scheme ("blade-slap") were investigated. These methods were based on using special rules for controlling the highest harmonics of a cyclic step in the general system of controlling the main rotor (method "HHC") [9].

The work presents the principal results of experimental research related to establishing a dependency of the helicopter tail rotor noise at axial streamline on its geometrical, kinematic and aerodynamic characteristics.

## **Object and test methods.**

Acoustic tests of tail rotor were carried out on the aerodynamic stand of M.L.Mil Moscow Helicopter Plant in February-June, 2000. The stand is a square room with dimensions of about  $13.5 \times 13.5 \text{ m}^2$ , in the centre of which a propeller device in the form of a tower of 5.3m in height is located (Fig.1). Along the perimeter the lower part of the concrete barrier has special windows of 2m in height, designed for free ejection of atmospheric air. The stand is supplied with an extensible roof.

The rotor axis in the experiment was vertical and the blade rotation plane was at a distance of 4.75m from the stand floor. The inductive flow from the rotor was directed upward. The distance between the rotor rotation axis and the stand walls

was 6.75m. The stand roof was moved sideways during tests.

A serial and a modified rotors of 3.9m in diameter were tested in 2-bladed and 3-bladed versions. The serial rotor blade was formed of symmetrical profiles of NACA 230M type and was rectangular in plane form, its chord value was 0.305m. The modified rotor blade was formed of non-symmetrical profiles of TsAGI CTM type, with constant chord value along the blade span (0.305m) and with sweep varying from  $8^\circ$  in the root section to  $0^\circ$  in the tip section (Fig.2). The modified blade has a more uniform distribution of aerodynamic loading in span. At  $C_T/\sigma = 0.15$  (loading parameter in Fig.2 is denoted as  $t_Y$ ) derivative value  $dt/dr$  achieves the highest value of the serial blade at  $r/R = 0.975$  and of the modified blade at  $r/R = 0.94$ .

The measured polars of the modified TR for 3-bladed and 2-bladed versions are presented in Fig.3 and 4. One can see that for the 3-bladed version there is a linear dependency of the blade loading parameter ( $C_T/\sigma$ ) on the normalized value of the sweeping momentum ( $m/\sigma$ ) and on the blade pitch angle varying in the range of  $9^\circ$ - $15^\circ$ . This proves the absence of separation phenomena in the 3-bladed rotor version at its operation in the considered range of pitch variation angles. In the case of 2-bladed version of the modified TR the measured aerodynamic polars are non-linear (Fig.4) and this proves a possible appearance of separated streamline of blades at pitch angles more than  $18^\circ$ . As the peripheral velocity Mach number increases, the separated phenomena are revealed more intensively.

Independent parameters of the propeller operation in the tests were the peripheral velocity and blade pitch angle. The thrust, sweeping momentum and sound pressure were measured in the tests.

Sound pressure measurement were made at two points of the acoustic near field of the tail rotor. Condensor microphones, type 4134 of B&K, were placed at a distance of 1.7m (point M1) and 6.83m (point M2) from the blade tip periphery, above the TR rotation plane, outside the inductive flow zone (Fig. 1). Microphone M2 was placed in free space. A straight line connecting the microphones, formed an angle of  $\sim 30^\circ$  to the TR rotation plane.

Signals from the microphones were supplied to sound meters of "RFT" and were recorded with the use of an analog 4-channel tape recorder of "Sony". Spectral analysis of the sound pressure was realized with the help of real time analyzers, type 2133 and 2034 of "B&K". The tests were carried out at the peripheral velocity Mach numbers of blade tips from 0.4 to 0.7 and at variations of TR blade pitch angle in the range of  $9^\circ$  -  $22^\circ$ .

It is known that in measurements of sound pressure in the acoustic near field of air propeller the measurement results much depend on phase relations of signals coming to the measurement point from radiation sources distributed in the TR rotation plane.

For an approximate evaluation of possible distortion in the near field of the source of sound pressure spectra which is associated with sound wave interference, difference interference spectra of sound pressure in 1/3-octave frequency bands were predicted for points M1 and M2 (Fig.1). The prediction was made for the following conditions: the blade tip part radiates sound; radiation of two blades located in azimuthes of  $180^\circ$  and  $300^\circ$  ( $0^\circ$  corresponds to the minimum distance from the blade tip to the point of sound pressure measurement) is taken into account simultaneously - in these azimuthes the largest difference of sound wave travel from two blades is realized; at the moment of simultaneous sound

radiation by two TR blades the signals have an identical intensity and initial phase.

The predicted difference interference spectra of sound pressure in 1/3-octave frequency bands are given in Fig. 5. The ordinate axis shows the difference between the overall sound pressure level produced by two sources and the sound pressure level produced by one of the sources.

It's known that due to summarizing two signals with an identical initial phase and a certain difference in travel there appears an interference picture characterized by a sequential position of the characteristic maxima (constructive interference) and minima (destructive interference) of sound pressure on the frequency scale (wave lengths). When the oscillation phases of sound pressure in two coming waves coincide, a pressure amplitude doubling and sound pressure level increase by 6 dB take place. When the signals come in the opposite phases, they can suppress each other and this manifests itself in the interference spectrum as a vigorous destructive gap in the respective frequency region. In the signal analysis in 1/3-octave frequency bands, the width of which is a final value and continuously increases with the central frequency, a significant number of oscillations with different phases is summarized simultaneously in each frequency band and their number is the greater, the higher is the central band frequency. As a result, starting with a central frequency band, the waves with random sets of phase difference take part in the interference and the case of energetic summarizing of signals is realized. This is revealed in the difference interference spectrum as an increase of sound pressure level from two sources by a value up to 3 dB.

The prediction results presented in Fig.5 show that even in the considered case of the largest distance between the sources relative to the point of sound pressure measurement the intensive interference manifests itself in a sufficiently

narrow frequency region of 50-250 Hz for both measurement points. At the frequencies higher than 250 Hz and lower than 40 Hz the value of interference correction is practically independent of frequency and hence, it will not depend on the rotor operation regime. This permits making a comparison between the results of sound pressure level measurements in the near field of TR at different operation regimes.

### **Principal measurement results.**

Below we consider an effect of rotor pitch ( $\varphi$ ) and peripheral velocity Mach number (M), an overall effect of aerodynamic profile and blade sweep, an effect of blade number ( $k_B$ ) and rotor thrust (T), a correlation of sound pressure level and aerodynamic parameter of blade loading ( $C_T/\sigma$ ) on TR noise spectrum at axial streamline.

The foundation of air propeller aerodynamic noise is determined and random processes characterizing a force interaction between the blades and environments. This interaction is realized in the process of transformation of the blade rotation energy into the medium movement energy through the rotor disk and when the hard blade body is passing through elastic air environments. According to the accepted terminology, a common acoustic radiation of air propeller is subdivided into rotation noise and vortex noise. The first one is determined by blade force effect on the medium, the second is connected with radiation from the turbulent boundary layer on the blade surface and from the blade wake. In its turn, the rotation noise includes the aerodynamic noise of loading and the displacement noise.

TR of the helicopter of single-rotor scheme functions in the turbulent medium and is a source both of harmonic noise components of TR rotation and of broadband noise of vortical generation.

Investigations of broadband noise of the isolated helicopter rotor on stands and in wind

tunnels have shown that the interaction between a rotor blade and random non-uniformities in the advancing flow is one of the effective sources of vortex noise. This interaction causes a fluctuation of the blade section angle of attack and as a result, a fluctuation of the aerodynamical load affecting the blade. Periodical fluctuations of the aerodynamical load, normal to the profile surface, near its trailing edge, which involve vortex convergence and formation of a vortex sheet following the blade, are the sources of vortex noise.

The noise of vortical generation appears also due to the pressure fluctuation field formation on the blade surface, caused by the turbulent boundary layer (BL), at BL separation from the blades and also due to pressure fluctuations in the turbulent wake, following the blade.

If the rotor operates in the undisturbed medium at axial streamline, the blade loading in the connected coordinate system is of stationary character. However, in this case, near the trailing edge of the profile there is also a fluctuation of the aerodynamic load normal component, which involves vortex convergence and vortex sheet formation. Sound radiation is determined by blade rotation, i.e. by a periodical effect of stationary load on the boundary space region (rotation noise) and by a trailing edge noise (vortex noise).

The experimental research realized within the limits of the present work relates to TR acoustic field at axial streamline. This permits some refinements of the role and the frequency characteristic of separate sources of vortex noise in the common noise of TR to be introduced as well as of the dependency of TR noise intensity on its geometric and kinematic parameters.

#### **Effect of peripheral velocity and rotor pitch.**

Processing of the sound pressure measurement results has shown that the pressure

realization in time, measured in the near field of TR, includes both periodical and continuous (random) components. For all the values of peripheral velocity Mach number considered ( $M=0.4-0.7$ ) the rotor pitch increase produces a noticeable growth of the random noise component amplitude. In this case the amplitude and shape of the periodical pressure component enveloping are somewhat changed.

For the values of the rotor blade pitch angles from  $9^\circ$  to  $14^\circ$  the peripheral velocity Mach number increase leads to a noticeable increase of the periodical pressure component amplitude. Since the random pressure fluctuations correspond to a broadband component in the radiation spectrum and the periodical fluctuations correspond to harmonic components in the radiation spectrum, one can draw a conclusion that the rotor pitch variation leads, at least in the region of a linear area of the polar, to variations of the broadband radiation spectrum part and the peripheral velocity Mach number variation leads to transformation of harmonic components of TR radiation spectrum. This conclusion is supported by 1/3-octave sound pressure spectra measured in the near field of TR.

Fig.6 presents in its upper plot the 1/3-octave sound pressure spectra of the modified 3-bladed rotor at the peripheral velocity Mach number 0.6 for different blade pitch angles, measured at point M1. The lower plot shows the values of rotor efficiency and the levels of first five harmonics of the periodical component of rotor noise, according to a blade pitch angle. As follows from the rotor polars considered above, the blade pitch angle increase at  $M=\text{const}$  within the limits of a linear area of the polar causes an increase of rotor thrust without affecting the blade streamline character. At large blade pitch angles corresponding to a non-linear area of the polar, the rate of thrust increase is reduced due to formation of flow separation zones on the upper blade surface.

From the sound pressure spectra presented in Fig.6 one can see that rotor pitch increase from 9° to 15° leads to a noticeable, up to 10 dB, increase of broadband noise at the frequencies higher than 250 Hz. At the frequencies lower than 250 Hz the sound pressure level in a 1/3-octave frequency band is determined by harmonic noise component contribution. The rotor pitch increase in the 3-bladed version caused a significant, up to 10 dB, increase of noise level at the blade passage frequency (the first harmonic of rotation noise). The levels of harmonics from the second to the fifth vary insignificantly in this case.

Since the rotor operation regime changed in the polar linear area and the rotor efficiency in this polar area monotonously increased with the rotor pitch, one can assume that the broadband radiation source of the 3-bladed modified rotor in the frequency region higher than 250 Hz is of vortical generation and is not associated with flow separation.

Along with this, in the case of the modified rotor in 2-bladed version, the blade pitch angle increase leads to non-linear variation of the efficiency (Fig. 7, lower plot); at  $\varphi > 16^\circ$  the efficiency begins to decrease sharply. The efficiency decrease is accompanied by an increase of harmonic components of the rotor noise with the harmonic numbers 3 and 4. It is important that the broadband noise intensity also decreases in the frequency range of 300-1000 Hz as the rotor efficiency decreases, but in the high frequency range (above 2000 Hz) this effect is not observed, however.

One can speak about the existence of different mechanisms of broadband noise in the regions of middle and high frequencies. Since the rotor efficiency decrease at high pitch values usually is determined by appearance of flow separation regions in the root and tip blade parts and by reduction of its carrying ability, one can assume that the broadband radiation in the middle

frequency region is connected with aero-dynamic force fluctuations caused by formation of separated zones on the upper blade surface.

It is known that the frequency maximum in the sound pressure spectrum of vortex noise can be found from the relations for the process homochronuity criterium (Strouhal number) which is the following for the helicopter rotor:  $Sh = f_{max} \times c / \{(wR) \times (1 + \mu)\}$ , where “c” is the thickness of the blade aerodynamic profile, “ $\mu$ ” is the parameter of the rotor operation regime ( $\mu = 0$  for the case of axial streamline),  $Sh = 0.2-0.4$  is the Strouhal number value for the noise of vortical generation, “ $f_{max}$ ” is the maximum frequency in the sound pressure spectrum. For the tail rotor considered the middle value of “ $f_{max}$ ” is  $\sim 1800$  Hz, if we assume  $\bar{c} = 11\%$  and  $wR = 200$  m/s, and in our case this corresponds to the high frequency component of vortex noise.

The peripheral velocity Mach number variation in the range of 0.4-.7 practically has no influence on the effect noted above.

### **Thrust effect.**

According to the semi-empirical model of helicopter rotor noise [10], the acoustic radiation power of the rotor, produced by a steady component of the aerodynamical loading, is expressed as follows:

$$W_{st} \sim (\rho / a_0^3) \times M^2 \times k_B^2 \times (C_T / \sigma)^2 \times (wR)^6 \times A_B, \quad (1)$$

or with the use of the expression through the rotor thrust ( $T_{TR}$ ):

$$W_{st} \sim (\rho / a_0^3) \times (T_{TR}) \times k_B^2 \times (C_T / \sigma) \times (wR)^4, \quad (2)$$

where  $\rho$  is the air density,  $a_0$  is the ambient sound speed,  $C_T / \sigma$  is the parameter of rotor blade loading,  $k_B$  is the blade number,  $A_B$  is the area of the blade surface,  $M$  is the peripheral velocity Mach number.

The evaluation of rotor parameter effect on the radiation noise intensity was made on the basis of data analysis in linear ( $L_C$ ) and in weighted ( $L_A$ ) overall levels of sound pressure. The value of  $L_C$

indicates an overall intensity of all the spectral components, both harmonical and broadband in the frequency range of 50-10000 Hz, and the value of  $L_A$  shows an intensity of noise components in the frequency range higher than 300 Hz, i.e. generally, in the broadband component.

The experimental data on the rotor thrust effect on the normalized value of the overall sound pressure level in the near field of the serial 3-bladed rotor at the peripheral velocity Mach number 0.4 are presented in Fig. 8 for noise measurement points M1 and M2. The upper and middle plots on the ordinate axis indicate the following value:

$$\Delta L = L_i - L_0 - 10 \lg (C_T / \sigma), \quad \text{dB, dBA.}$$

where  $L_i$  is the linear or weighted overall sound pressure level for the current rotor thrust value,  $L_0$  is the overall sound pressure level at TR thrust of 190 kg (for the upper plot in Fig.8) or at the peripheral velocity Mach number 0.4 (for the middle plot in Fig.8).

The upper plot in Fig.8 shows that the thrust variation occurs only at the expense of rotor pitch increase and the middle plot presents the data relating to a fixed thrust of 500-580 kg.

It can be noted that  $\Delta L_A$  dependency on rotor thrust (for the weighted overall sound pressure level) is close to a linear one in Fig.8 (upper plot). Thrust increase from 190 kg to 440 kg leads to  $\Delta L_A$  increase by 3 dBA at both noise measurement points. This corresponds to the broadband rotor noise intensity dependency on thrust in the form of  $W \sim T^k$  at  $k = 0.82$ .

Previously, at least two different mechanisms of broadband noise generation by tail rotor were set: in the middle-frequency range and in the high-frequency range. In the high-frequency range the radiation intensity varies monotonously at rotor thrust variations and in the middle-frequency range this monotony is broken due to appearance of flow separation regions on the upper blade

surface. It is possible that exactly due to this superposition of radiations from different sources the index value of degree "K" turned out to be 0.82 and not 1, as it should be according to expression (2).

As to the linear overall sound pressure level variation, different results are obtained for measurement points M1 and M2. Close to the rotor rotation plane (point M1) dependency  $\Delta L_C$  on the rotor thrust is more strong, than it is far from the rotation plane (point M2). The overall noise intensity of TR for point M2, as well as the intensity only of the broadband noise component, is proportional to the rotor thrust.

The middle plot of Fig.8 presents  $\Delta L_C$  and  $\Delta L_A$  dependencies on the peripheral velocity Mach number for the serial 3-bladed rotor at points M1 and M2. For  $\Delta L_A$  these dependencies at points M1 and M2 are close to each other and for  $\Delta L_C$  they are different. The peripheral velocity Mach number variation in the range of 0.4-0.7 leads to increasing of the normalized weighted intensity level ( $\Delta L_A$ ) by  $\sim 7$  dBA and this corresponds to dependency  $W \sim M^{3.3}$ . In this case the normalized linear overall sound pressure level ( $\Delta L_C$ ) at point M1 varies over  $\sim 0.4$  dB and this corresponds to the following noise intensity  $W \sim M^{4.8}$ .

According to expression (2), the rotation noise intensity must be proportional to the product of thrust by Mach number to the 4-th power:  $T^1 \times M^{4.8}$ . The experimental data obtained correspond to dependencies:  $T^{0.82} \times M^{3.3-4.8}$  and this can be considered a satisfactory experimental confirmation of predicted relation (2).

The lower plot of Fig.8 presents the data relating to the normalized linear overall sound pressure level dependency on rotor thrust for 4 values of the peripheral velocity Mach number in the range of 0.4-0.7 for a serial 3-bladed rotor. Within the data presented for each M-number, the blade pitch angle varied in the range of 9°-14°.

The data relating to different Mach numbers can be kept, to one dependency, if a correction for Mach number is introduced in the experimental data, as follows:  $10\lg(M/0.4)^4$ . In this case the data relating to  $M=0.5$ ;  $0.6$ ;  $0.7$  decrease by 3.9 dB, 7 dB and 9.7 dB, respectively, and together with the data for  $M=0.4$  they will form a unified monotonous non-linear dependency  $\Delta L_C = f(T)$ . At small Mach numbers ( $M=0.4$ ) the rotor noise intensity is proportional to  $T^{1.33}$  and at  $M=0.7$  - to  $T^{1.75}$ . An additional, in comparison with  $T^1$  rule, increase of noise intensity which takes place, as the peripheral velocity of rotor increases, can be determined, for example, by manifestation of wave effects appearing at Mach numbers, close to the critical value for a given profile or exceeding it.

#### **Loading parameter effect.**

The loading parameter effect ( $C_T/\sigma$ ) on the linear overall sound pressure level value in the near field of TR is shown in Fig.9, where the normalized overall sound pressure level (OSPL) dependency on the loading parameter is presented for a modified tail rotor with 2 and 3 blades. The OSPL are normalized in the peripheral velocity and the blade surface area, according to the relation composed of expression (1):

$$dL = SPL - 60\lg(wR) - 10\lg A_B, \text{ dB}$$

It can be noted that the experimental data are well correlated with the loading parameter for the 2-bladed and 3-bladed versions of modified rotor and the peripheral velocity Mach numbers considered.

#### **Blade number effect.**

It is of interest to evaluate the blade number effect on rotor noise. In comparison between the acoustic characteristics of rotors with different blade numbers one usually proceeds from the condition of providing unvariable thrust. The

condition of thrust constancy can be realized in different ways at the expense of varying geometrical and kinematic parameters of rotor on the basis of the following relation for thrust:

$$T = [\rho \times (wR)^2 / 2] \times (C_T / \sigma) \times k_B \times r \times b,$$

where  $r$  and  $b$  are then span and chord of the rotor blade,  $\sigma = (k_B \times b) / (\pi \times r)$  is the coefficient of rotor filling.

To obtain the highest effect in rotor noise reduction due to increasing its blade number ( $k_B$ ), it is necessary first to decrease those of its parameters, on which the radiated noise intensity depends most of all. It is seen from comparison between relations (1) and (2), that TR noise intensity depends to the highest degree on the peripheral velocity value (as  $(wR)^6$ ) and on the blade loading parameter (as  $(C_T/\sigma)^2$ ). The peripheral velocity reduction in this case is more preferable for noise level reduction, if the loading parameter values correspond to a linear area of the rotor polar, i.e. the rotor operation regime is close to the regime of maximum efficiency.

The 2-bladed and 3-bladed rotors in our experiment had practically identical diameters and blade chords. Therefore, according to relation (4), for keeping thrust unvariable in case of blade number increase, it is necessary first to reduce the peripheral velocity value ( $wR$ ). In this case, since the coefficient of filling ( $\sigma$ ) does not change, the blade loading parameter value is to be also reduced. The measurement results for two values of the available thrust of the modified rotor are presented in table, were  $\Delta L = L_3 - L_2$ ,  $L_3$  is the sound pressure level of 3-bladed rotor,  $L_2$  is the sound pressure level of 2-bladed rotor. One can see, that going from the 2-bladed version to the 3-bladed one with a simultaneous reduction of the peripheral velocity of rotor and keeping unvariable the rotor diameter and its blade chord permits reducing the overall acoustic radiation intensity of rotor by 5.3-7.3 dB and the vortex noise intensity level by 3.7-4.5 dBA.

$k_b$	thrust (kg)	M	$\varphi$ (degree)	$C_T / \sigma$	efficiency	$L_C$ dB	$L_A$ dBA	$\Delta L_C$ dB	$\Delta L_A$ dBA
2	742	0.7	11	0.179	0.694	122.3	114		
3	776	0.6	12	0.169	0.699	117	110.3	-5.3	-3.7
2	1096	0.7	16	0.265	0.682	125.9	117.7		
3	1044	0.6	15	0.228	0.711	118.6	113.2	-7.3	-4.5

The results obtained well agree with the data on aircraft propeller noise in forward flight of a light propeller airplane [11]. The blade number increase from 2 to 3 at a simultaneous decrease of M-number of the relative tip flow velocity from 0.78 to 0.73 and at a certain decrease of the rotor diameter (from 1.9m to 1.87m) produced the aircraft noise level reduction by the value of 3.8 dBA.

If increasing the blade number, one keeps the peripheral velocity value unvariable and the thrust constancy is kept only at the expense of variation (reduction) of rotor pitch, there is practically no benefit in noise level reduction of the 3-bladed version at low thrust levels (500-580 kg) and at the thrust level more than 1000 kg the noise level reduction is not more than 3 dB in linear overall sound pressure level.

#### **Effect of aerodynamic profile and blade sweep.**

Here is a comparison between the experimental data on noise of the serial and modified rotor in 3-bladed version at the peripheral velocity Mach number of 0.6; 0.65; 0.7. The comparison results are presented in Figs. 10, 11, 12 and 13. It can be noted that at  $M=0.6$  and  $M=0.65$  the overall linear ( $L_C$ ) and weighted ( $L_A$ ) sound pressure levels of rotor with different profiles (TsAGI CTM for a modified rotor, NACA 230M - for a serial rotor) and blade planforms (with sweep and without it, respectively) and at identical thrust level are practically not different from each other (Figs. 10 and 11). At  $M=0.7$  (Fig.12) the rotor with swept blades is characterized by higher linear overall sound pressure levels (upper plot) and practically

by identical overall vortex noise levels with the serial rotor (lower plot).

The 1/3-octave sound pressure spectra of the serial and modified rotors (Fig.13) show in comparison, that the modified rotor has lower levels of the high-frequency vortex noise and higher levels of the 3-d and 4-th rotation noise harmonics (in the frequency range of 100-250 Hz). The lower levels of vortex noise for the modified rotor are explained by the fact that the modified rotor produces the thrust identical to that produced by the serial rotor at smaller blade pitches.

#### **Conclusion.**

The experimental investigation of the effect of principal geometric, kinematic and aerodynamic parameters on the helicopter tail rotor noise intensity at axial streamline and at variations of the peripheral velocity Mach number in the range of 0.4-0.7 was carried out.

The effects of rotor pitch, peripheral velocity Mach number, profile and blade sweep, on the acoustic radiation spectrum, on linear and weighted overall sound pressure levels were researched. It is found that there are different noise sources of vortical generation which radiate in the middle and high frequency ranges.

It is obtained experimentally that a 3-bladed rotor, in comparison with a 2-bladed one, at identical geometric blade parameters and identical thrust level can provide the linear OSPL reduction by the value up to 7.5 dB and the weighted OSPL reduction by the value up to 4.5 dBA.

The modified rotor, in comparison with a serial one, has practically the same linear and weighted overall sound pressure levels. Along with this, the modified rotor radiates the lower vortex noise levels in the high frequency region (higher than 2000 Hz) and higher levels of harmonic components of the rotation noise in the

region of low frequency (100-350 Hz). The vortex noise level reduction is explained by the fact that at identical thrust levels of the serial and modified rotor, the latter operates at smaller blade pitches.

### References.

1. International standards and recommended practice. Environment protection. Annex 16 to Convention on International Civil Aviation. Vol.1. Aviation Noise. ICAO, 3-d Edition, 1993.

2. Gutin L. Ya. On the sound field of rotating propeller. Zhurnal techn. fiziki, 1936, v.6, № 5, pp.899-909

3. Yudin Ye. Ya. On vortex noise of rotating rods. Zhurnal techn. fiziki, 1944, v.14, № 9, pp.561-567.

4. Lowson M.N., Ollerhead J.B. A theoretical study of helicopter rotor noise. J. Sound and Vibr., 1969, v.9(2), pp.197-222.

5. Leverton J.W. Twenty-five years of rotorcraft aeroacoustics: historical perspective and importance. J. Sound and Vibr., 1989, v.133(2), pp. 261-287.

6. Johnson W. Helicopter Theory, v.2, Princeton University Press, 1980.

7. Kozkevnikova I.K., Samokhin V.F. Noise sources of helicopter with tail rotor. Akustichesky zhurnal, 1994, v.40, № 6, pp.962-968.

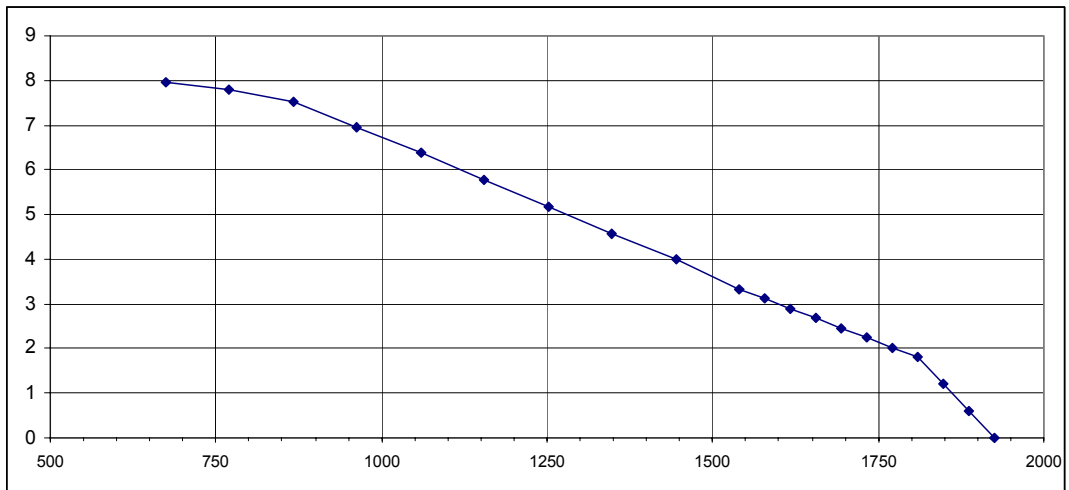
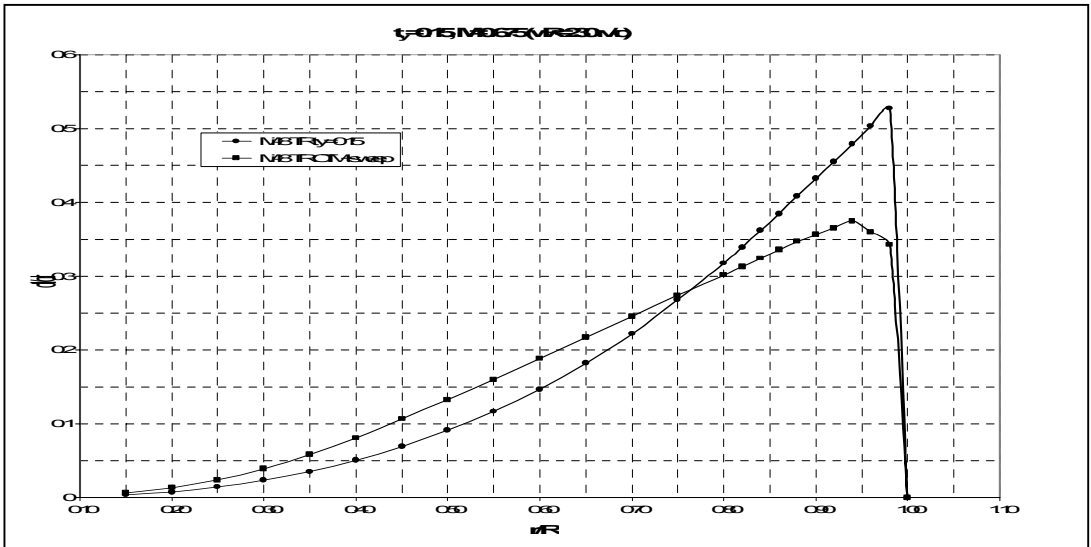
8. Samokhin V.F., Rozhdestvensky M.G. External Noise of Single Rotor Helicopters. AGARD Conference "Aerodynamics and Aeroacoustics of Rotorcraft" Proceedings № 552, Germany, 1994.

9. R. Kube, W.R. Spletstoesser, W. Wagner, U. Seelhorst, Y.H.Yu, A.Boutier, F.Micheli, E.Mercker. Initial Results from the Higher Harmonic Control Aeroacoustics Rotor Test (HART) in the German-Dutch Wind Tunnel. AGARD FDP Symposium "Aerodynamics and Aeroacoustics of Rotorcraft", Germany, 1994. AGARD-CP-552, 1995.

10. Samokhin V.F. Method of Community Noise Prediction for Helicopters of Single-Rotor and Coaxial-Rotor Scheme. TsAGI, Rep. №5591, 2000.

11. Hanno H. Heller. DLR. 5-th AIAA/CEAS Aeroacoustics Conference, 1999.





r/R	R	Fi	FiOTH
0.35	673.5	7.95	3.4
0.7	1347.5	4.6	0
1	1925	0	-4.6

Fig.2

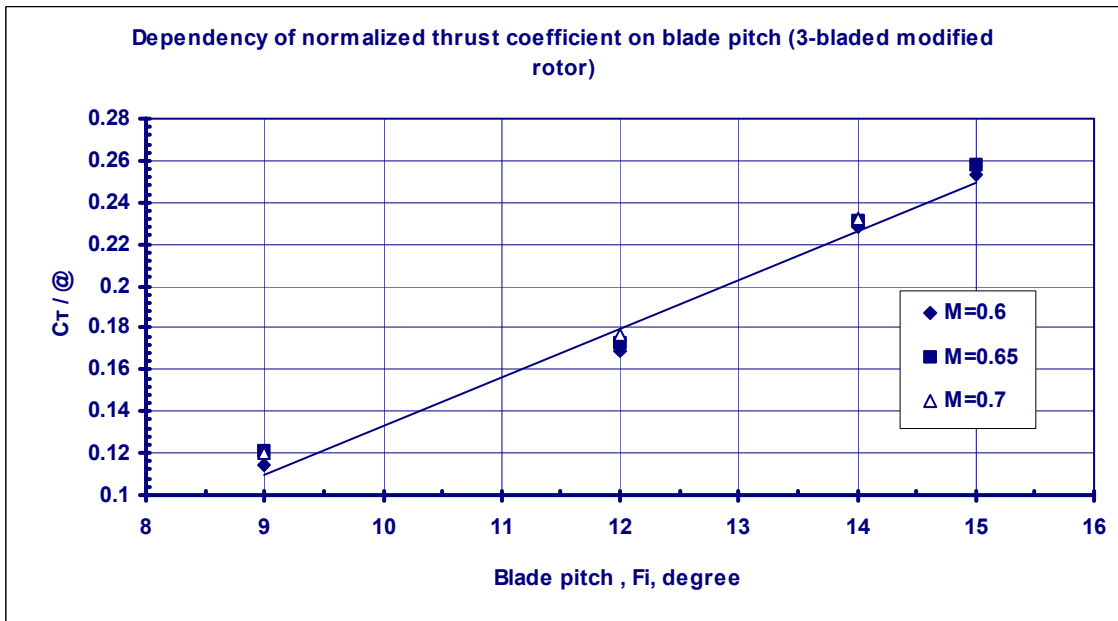
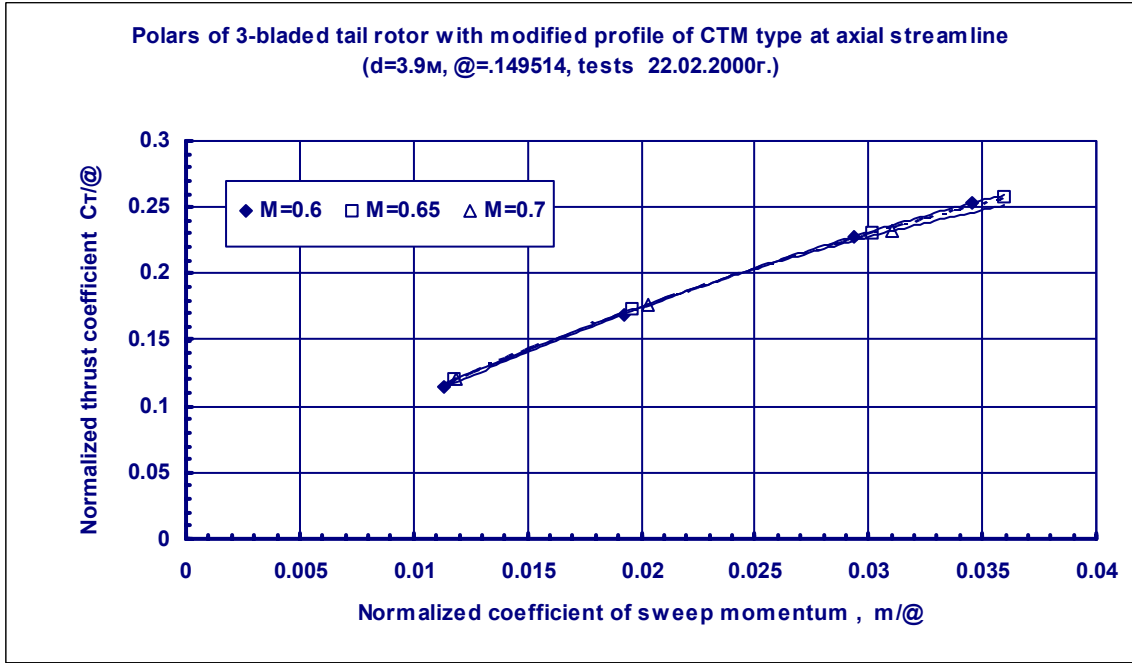


Fig.3

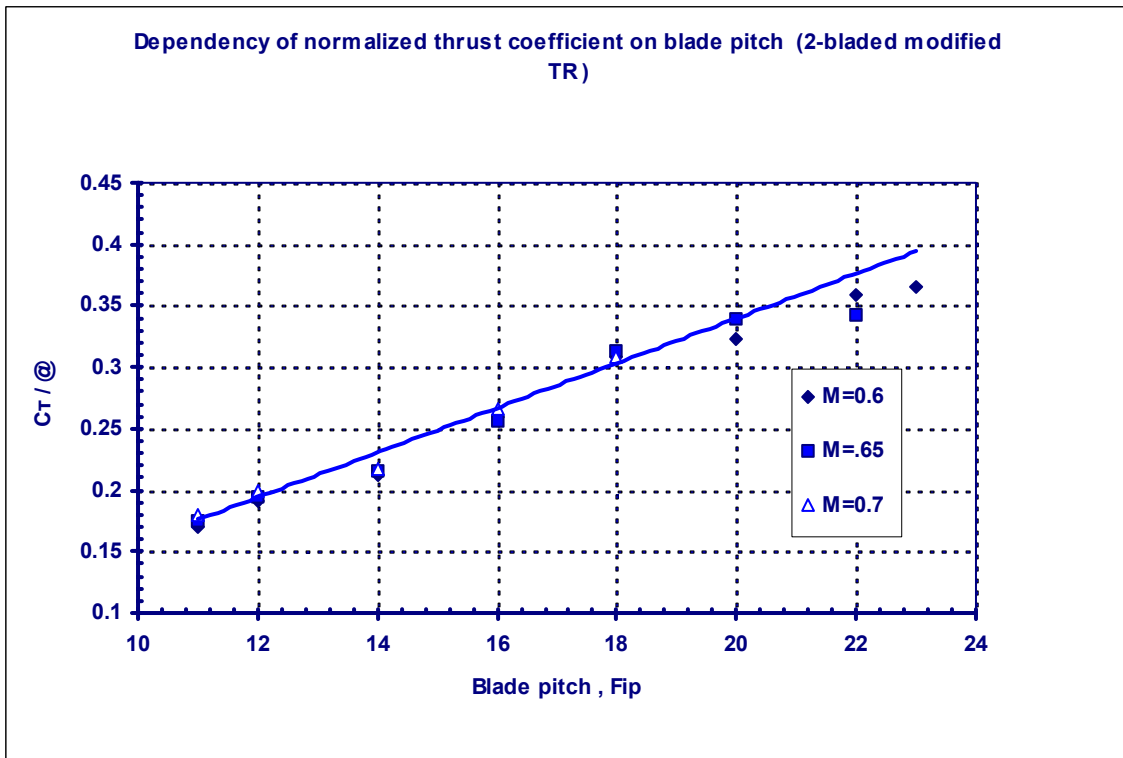
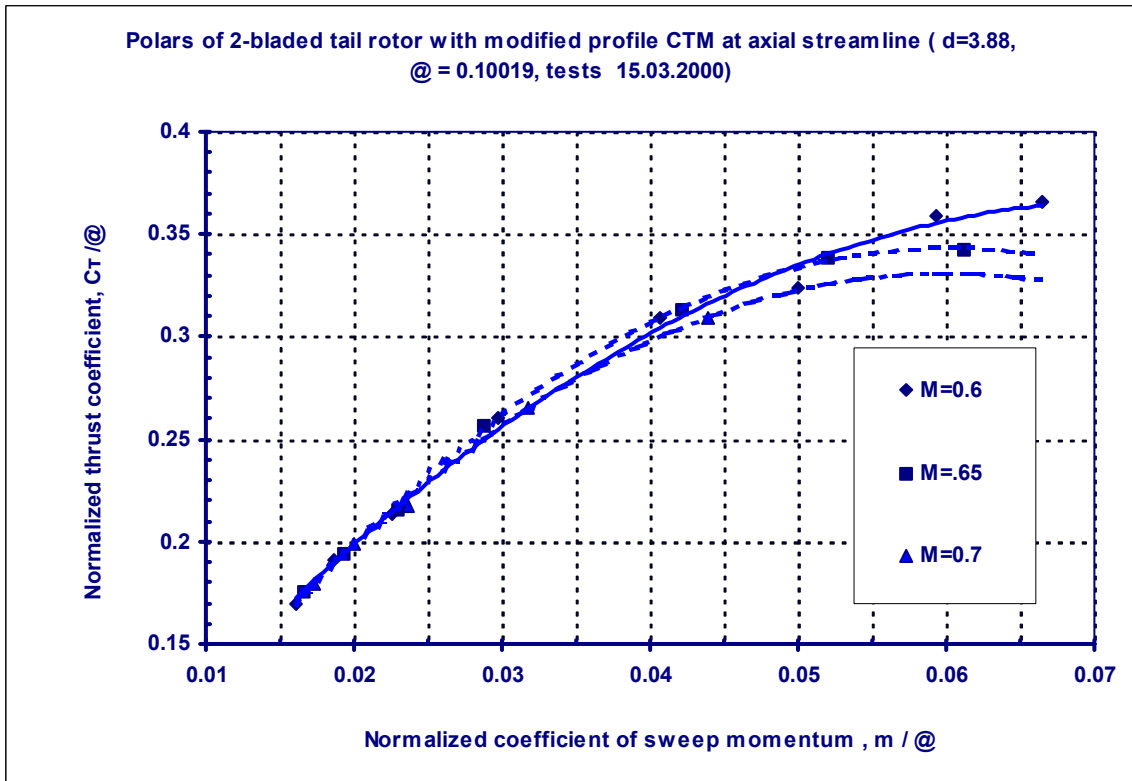
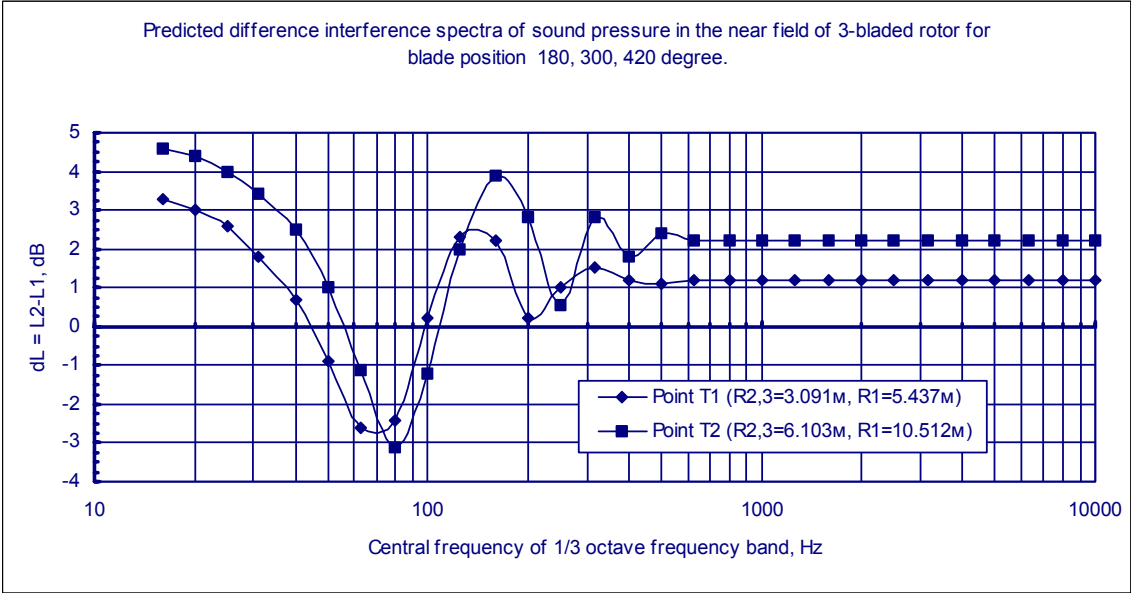


Fig.4



Prediction assumption: blade tip radiation;  
 radiation from 2 blades in azimuth 180 and 300 degree is considered;  
 signals are identical in intensity and phase at the moment of radiation;

**Fig.5**

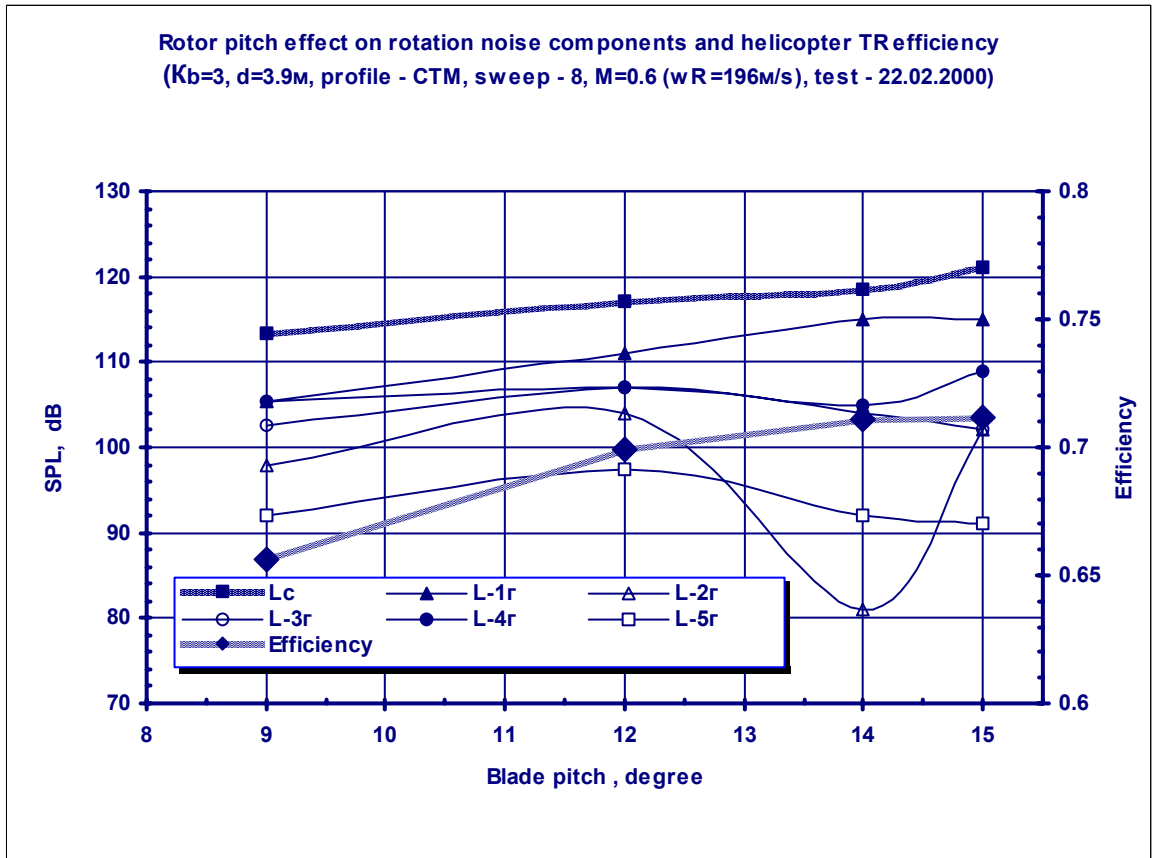
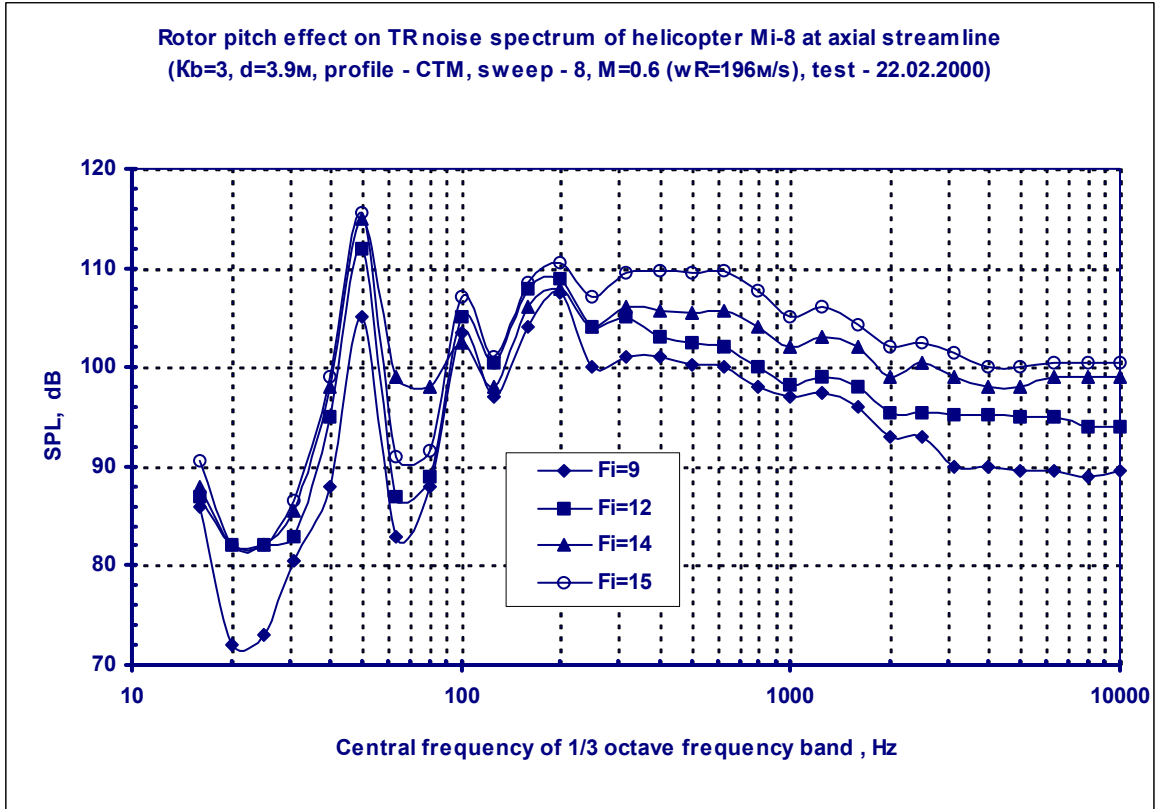


Fig.6

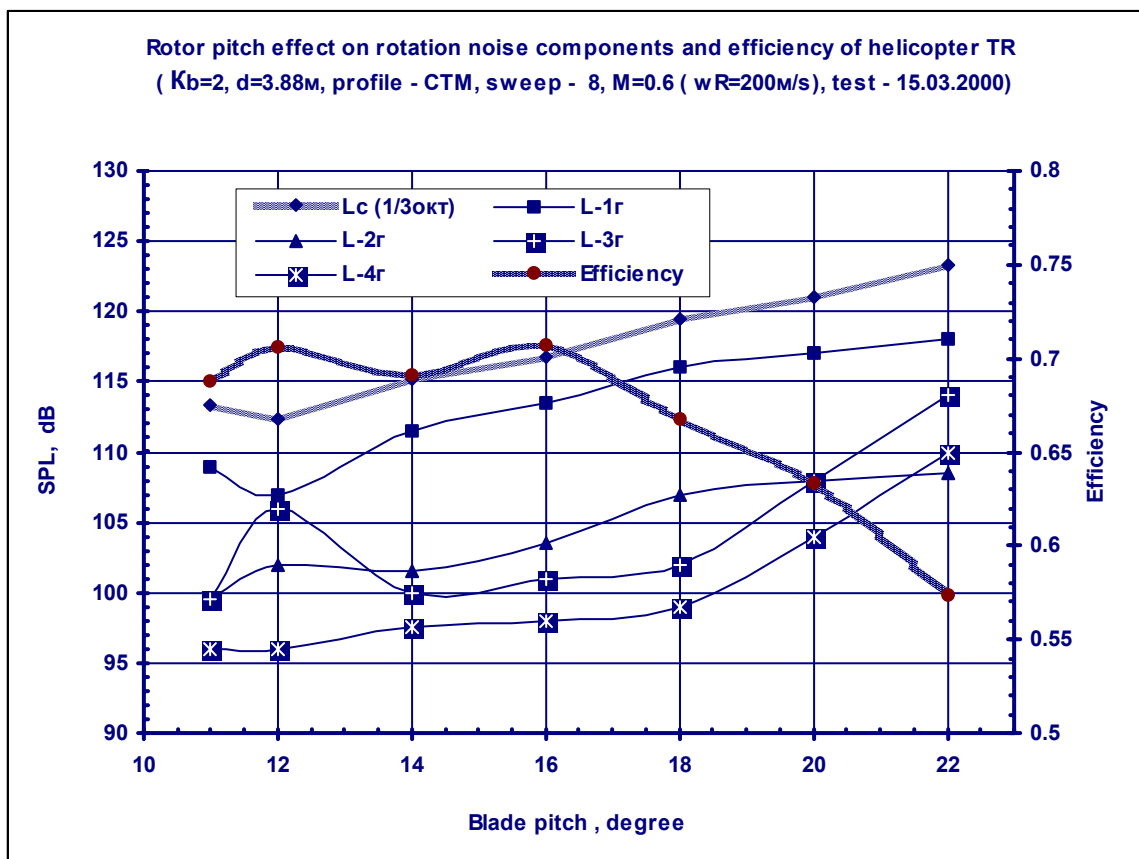
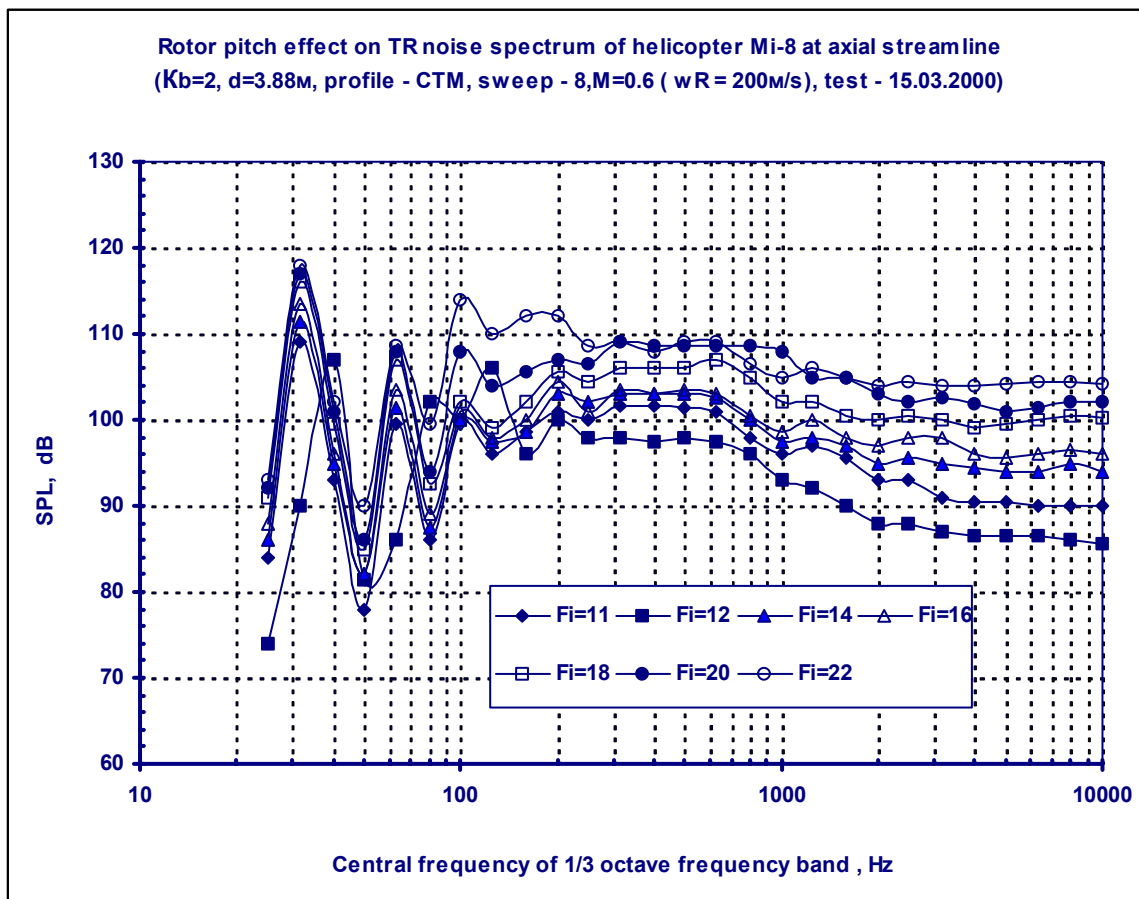


Fig.7

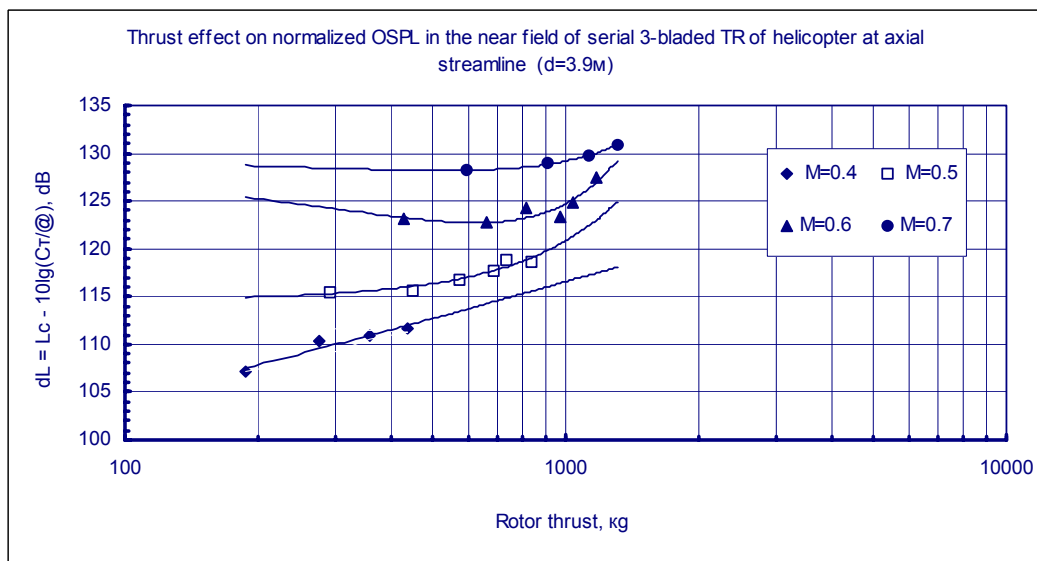
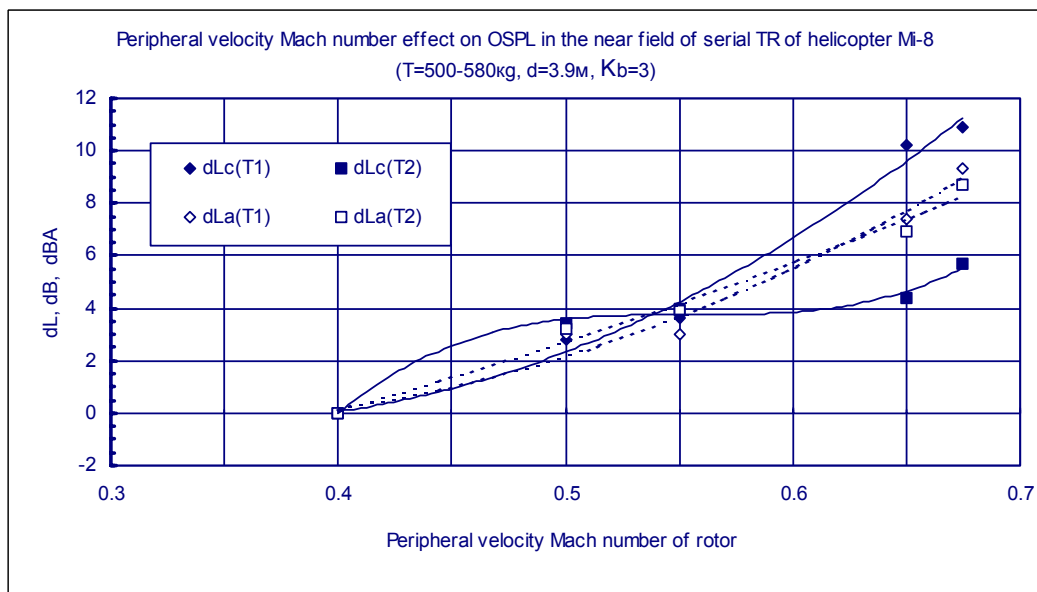
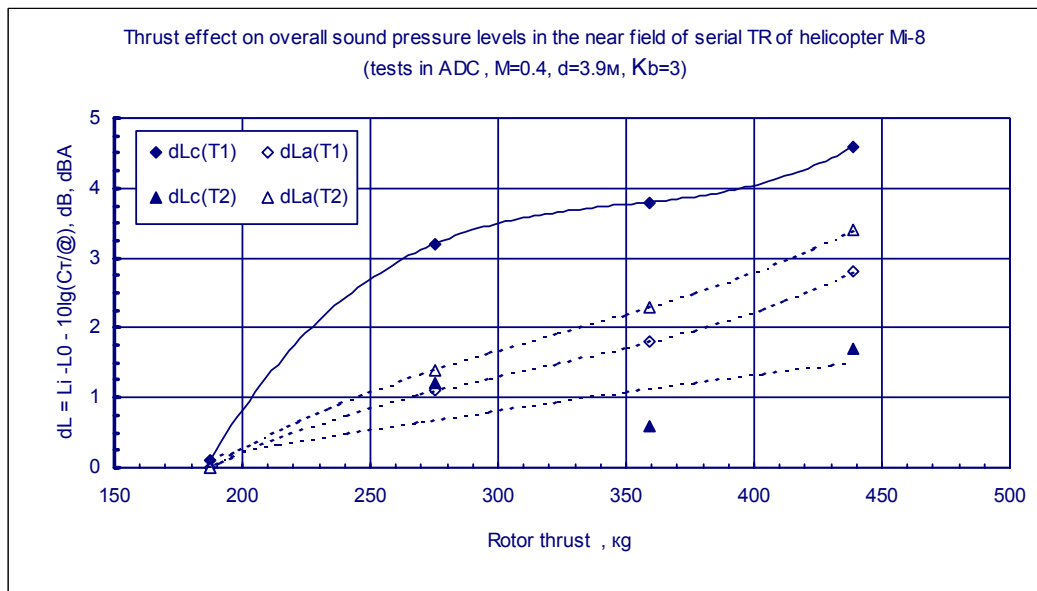
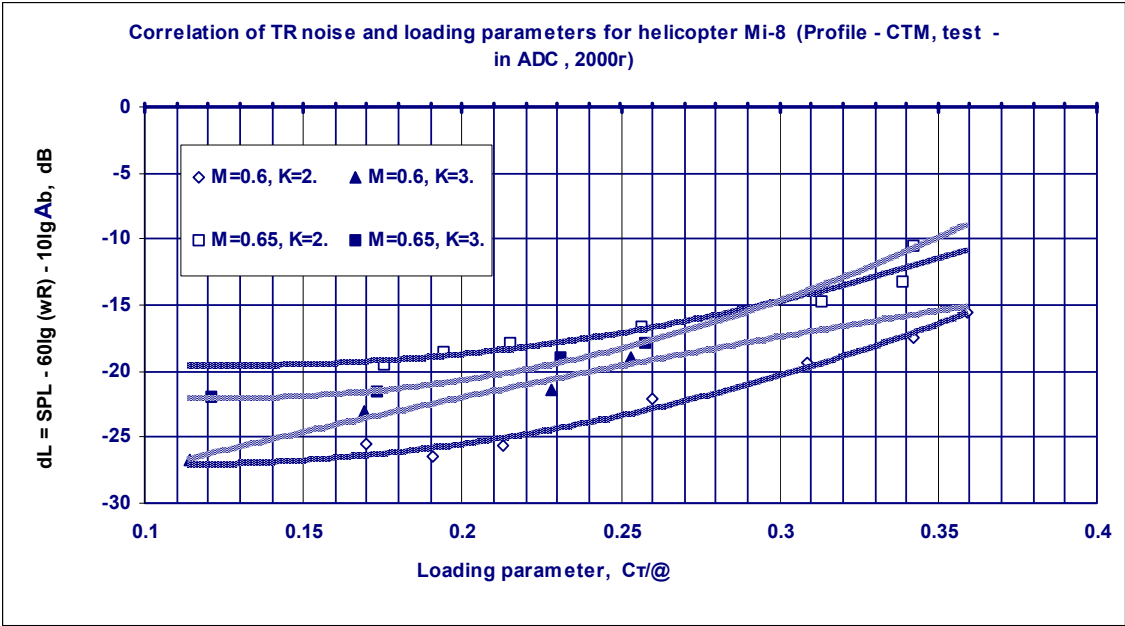
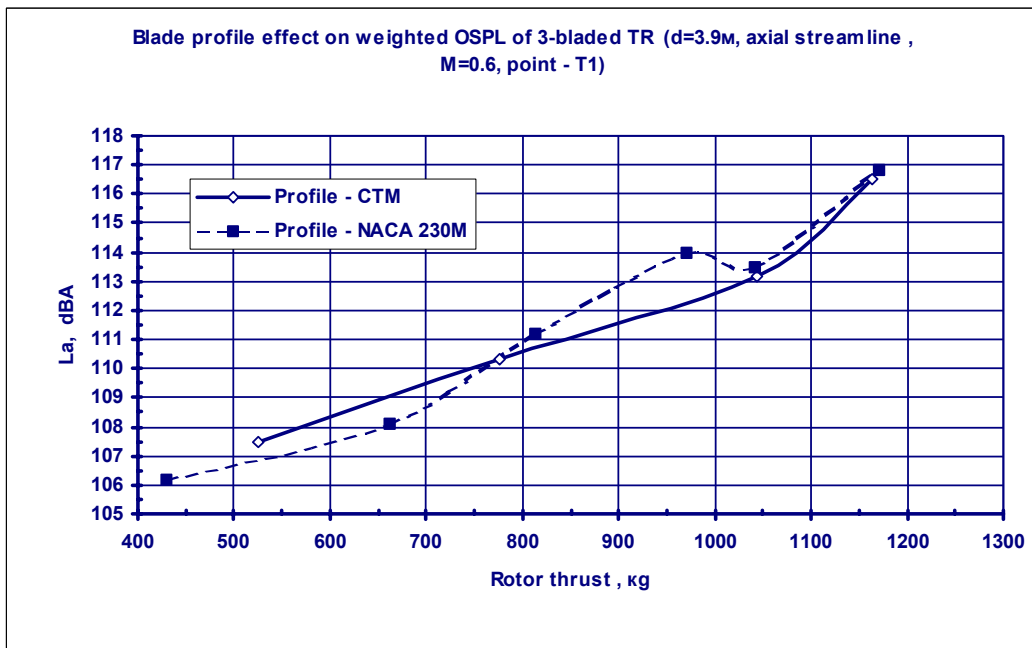
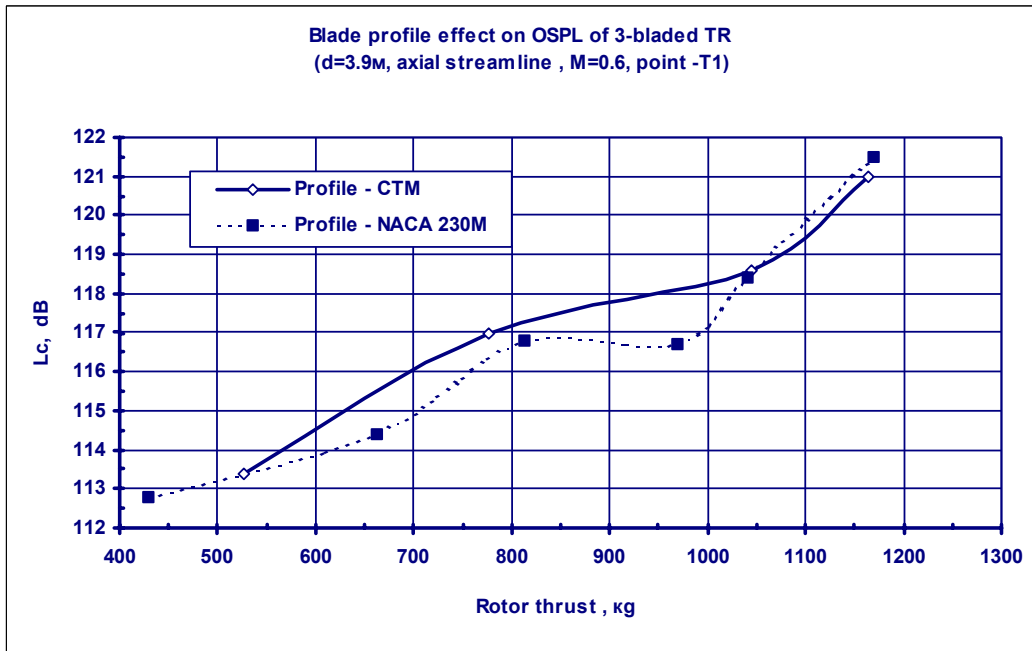


Fig.8



**Fig.9**



**Fig.10**

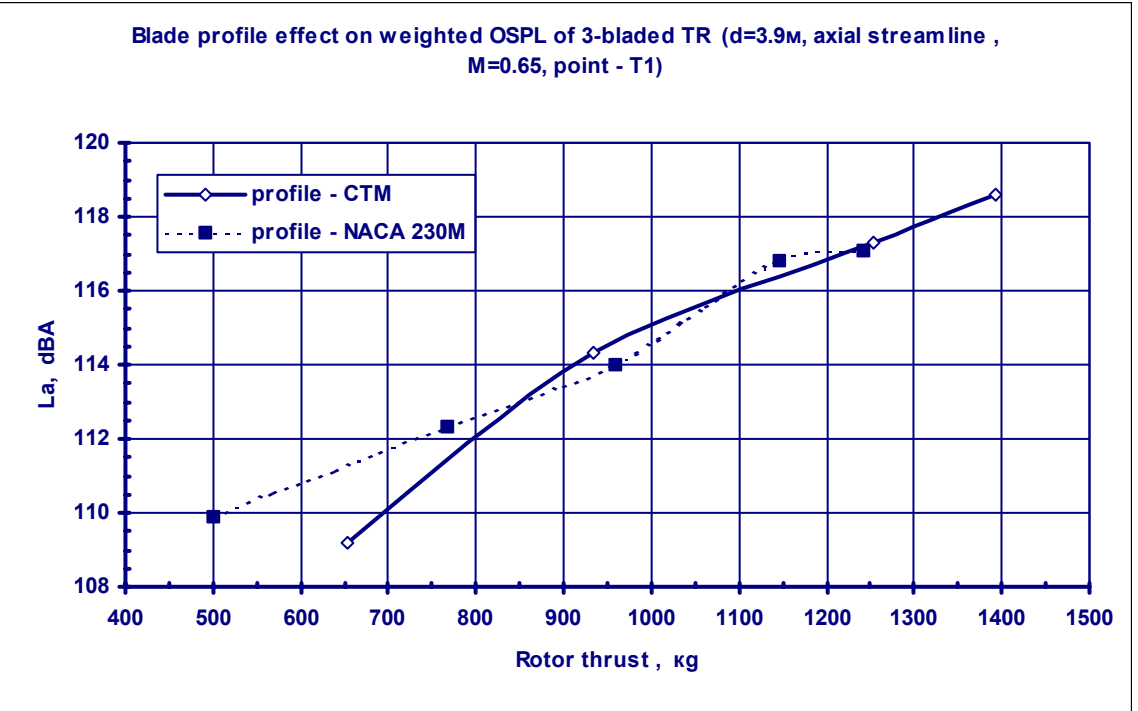
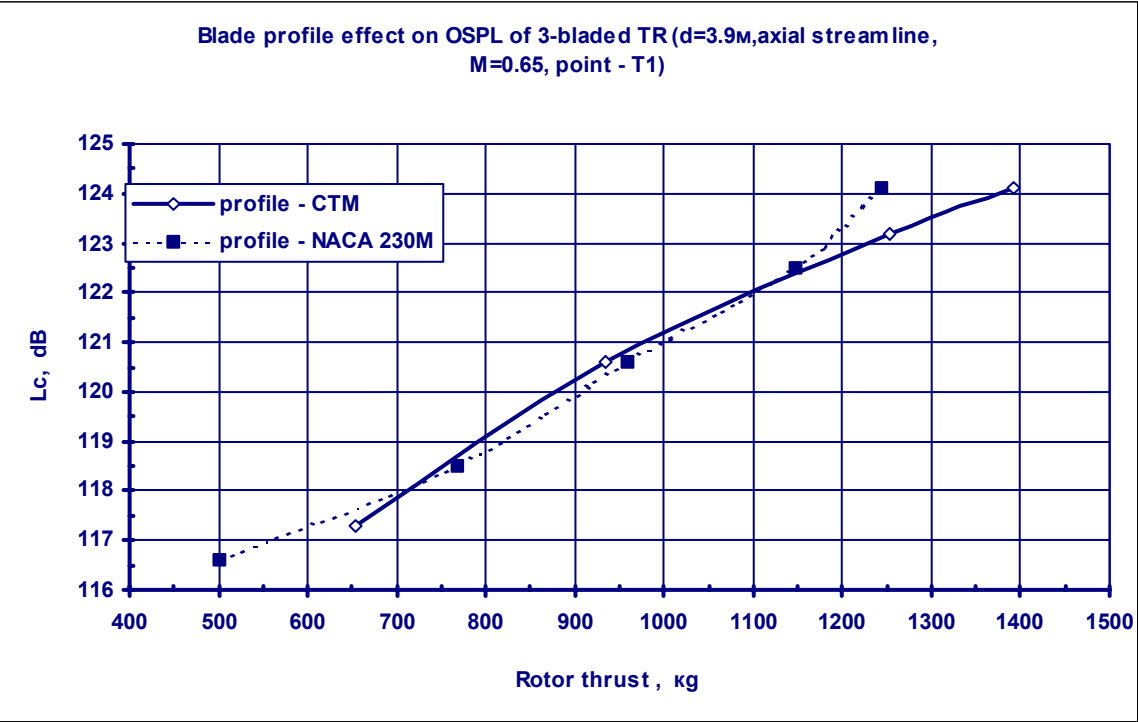


**Fig.11**

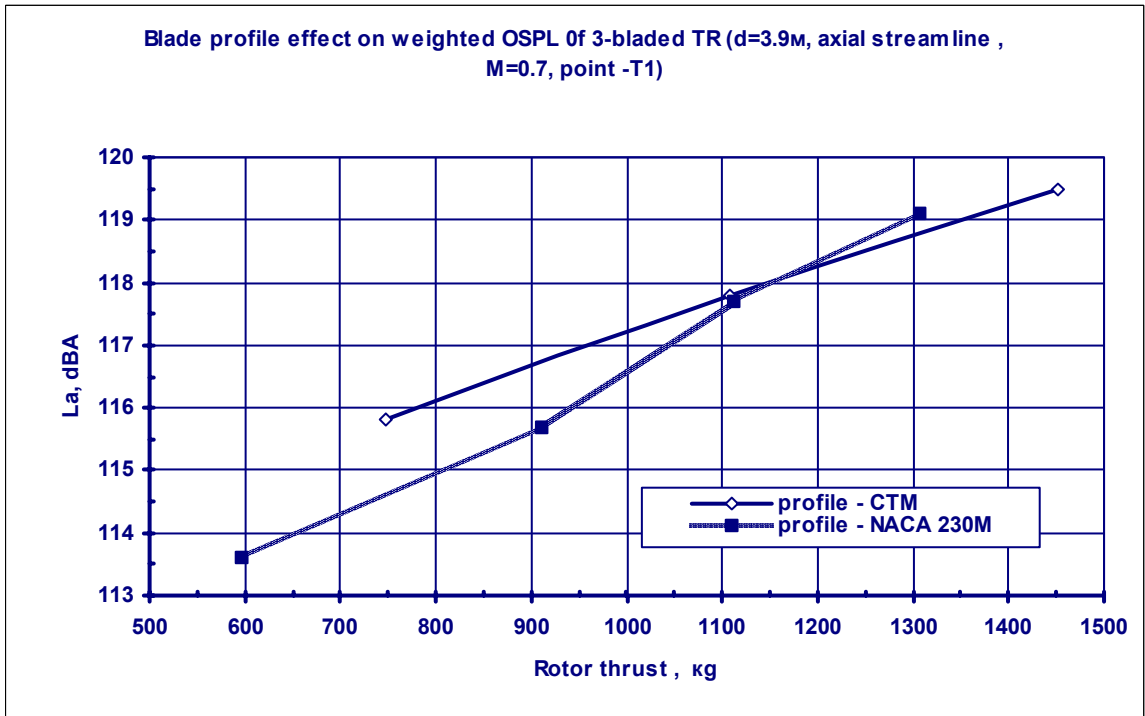
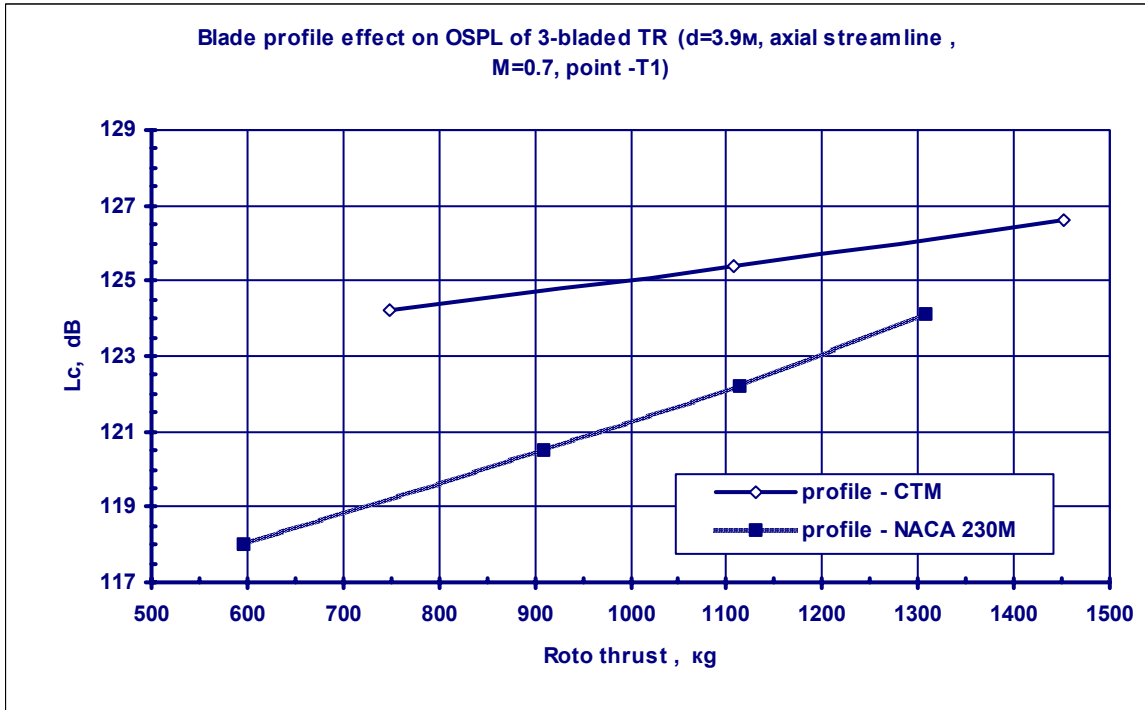


**Fig.12**

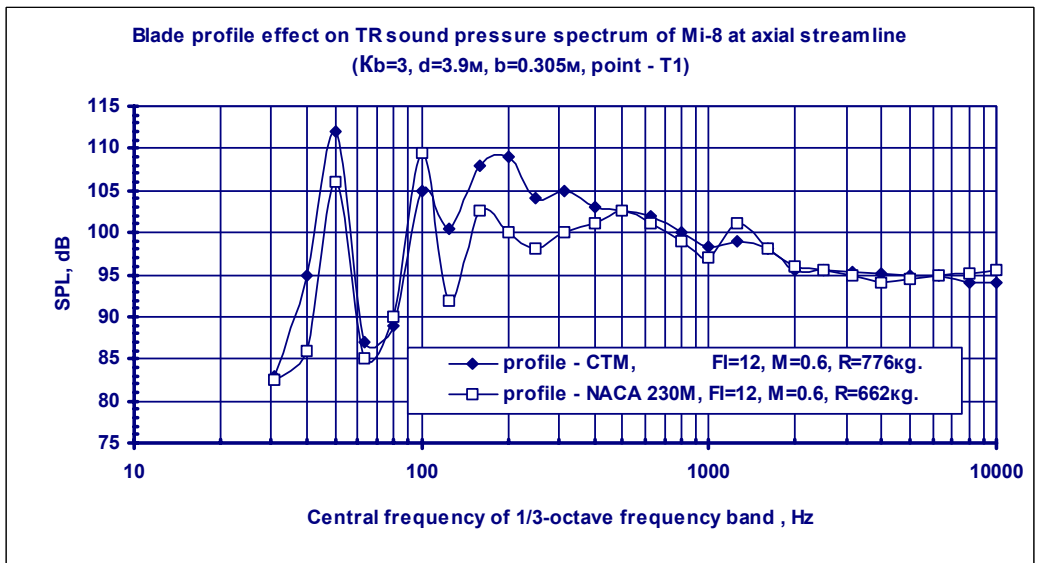
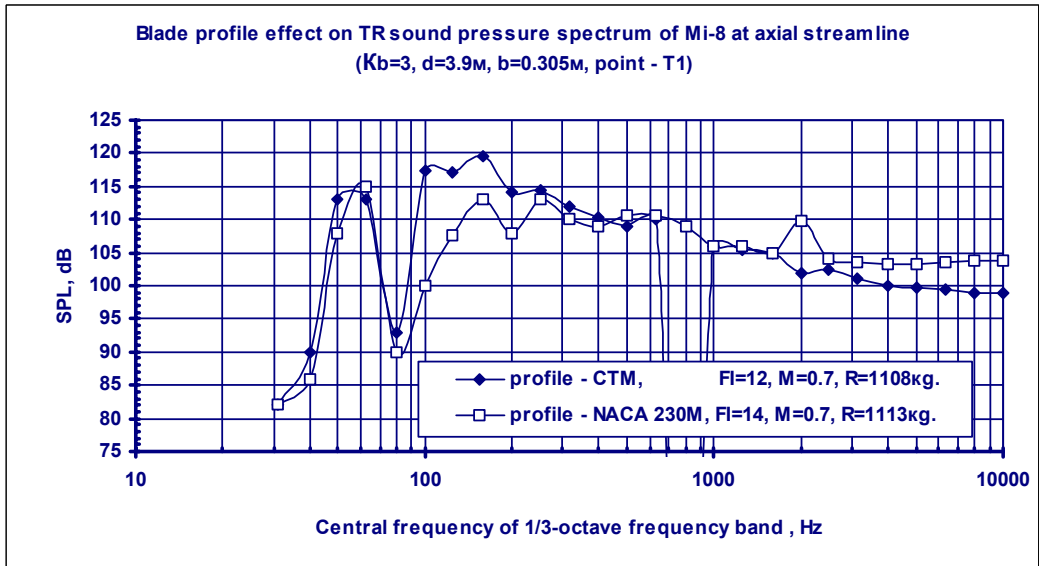
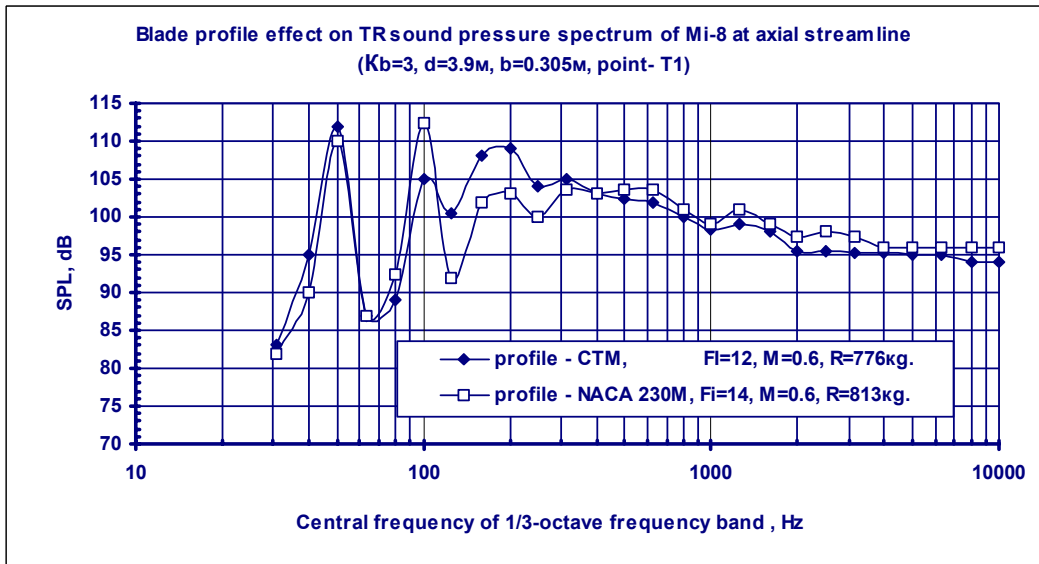


**Fig.13**